New Journal of Physics
The open access journal at the forefront of physics

Deutsche Physikalische Gesellschaft DPG IOP Institute of Physics

PAPER • OPEN ACCESS

Quantum metrology of solid-state single-photon sources using photon-number-resolving detectors

To cite this article: Martin von Helversen *et al* 2019 *New J. Phys.* **21** 035007

New Journal of Physics
The open access journal at the forefront of physics

Deutsche Physikalische Gesellschaft DPG
IOP Institute of Physics

Published in partnership with: Deutsche Physikalische Gesellschaft and the Institute of Physics

OPEN ACCESS

RECEIVED
11 October 2018

REVISED
20 December 2018

ACCEPTED FOR PUBLICATION
11 February 2019

PUBLISHED
28 March 2019

PAPER

Quantum metrology of solid-state single-photon sources using photon-number-resolving detectors

Martin von Helversen[1], Jonas Böhm[1], Marco Schmidt[1,2], Manuel Gschrey[1], Jan-Hindrik Schulze[1], André Strittmatter[1,3], Sven Rodt[1], Jörn Beyer[2], Tobias Heindel[1] and Stephan Reitzenstein[1]

[1] Institut für Festkörperphysik, Technische Universität Berlin, D-10623 Berlin, Germany
[2] Physikalisch-Technische Bundesanstalt, Abbestraße 2-12, D-10587 Berlin, Germany
[3] Present address: Institut für Experimentelle Physik, Otto-von-Guericke Universität Magdeburg, PF4120, Magdeburg, Germany

E-mail: tobias.heindel@tu-berlin.de

Keywords: quantum metrology, single-photon sources, photon-number-resolving detectors, transition-edge sensors, qantum dots

Abstract

Quantum-light sources based on semiconductor quantum dots (QDs) are promising candidates for many applications in quantum photonics and quantum communication. Important emission characteristics of such emitters, namely the single-photon purity and photon indistinguishability, are usually assessed via time-correlated measurements using standard 'click' detectors in Hanbury Brown and Twiss or Hong-Ou-Mandel (HOM-) type configurations. In this work, we employ a state-of-the-art photon-number-resolving (PNR) detection system based on superconducting transition-edge sensors (TESs) to directly access the photon-number distribution of deterministically fabricated solid-state single-photon sources. Offering quantum efficiencies close to unity and high energy resolution, our TES-based two-channel detector system allows us to analyse the quantum optical properties of a QD-based non-classical light source. In particular, it enables the direct observation of the two-particle Fock-state resulting from interference of quantum mechanically indistinguishable photons in HOM-experiments. Additionally, comparative measurements reveal excellent quantitative agreement of the photon-indistinguishabilities obtained with PNR ((90 $\pm$ 7)%) and standard click ((90 $\pm$ 5)%) detectors. Our work thus demonstrates that TES-based detectors are perfectly suitable for the quantum metrology of non-classical light sources and higlights appealing prospects for the efficient implementation of quantum information tasks based on multi-photon states.

1. Introduction

The dawn of quantum technologies is expected to revolutionize the fields of sensing, computing, and secure data communication [1]. Many concepts in quantum photonics and communication thereby rely on non-classical light sources emitting single indistinguishable photons at a given wavelength. Consequently, huge efforts have been directed towards the development of such light soures [2]. At the same time the metrology of quantum emitters has gained increasing importance [3, 4]. In particular, accurate measurements of the fundamental properties of light states, i.e. the photon emission statistics and the photon indistinguishability, are extremely important figures of merit to evaluate the quantumness of the emitters. To date, the majority of experiments still use single-photon counting modules (SPCMs) based on avalanche photodiodes or superconducting nanowires. These types of detectors are also referred to as 'click' detectors, as the absorption/detection of a single photon results in a change of the SPCM output state from 0 to 1 followed by a deadtime, where photon detection is not possible. As a consequence, click detectors cannot distinguish the number of photons present in a light field at a given time and therefore offer limited capabilities for the metrology of quantum-light sources. Due to the lack of practical detectors offering true photon-number-resolution, workarounds have been pursued using for instance click detectors in combination with cascaded beamsplitters [5, 6]. On the other hand, huge progress has been achieved in the development of truly photon-number-resolving (PNR) detectors [7, 8]. To date, the best performance with respect to photon-number-resolution and detection efficiency can be achieved with

superconducting transition-edge sensors (TESs) [9]. Using this type of detector, Di Giuseppe *et al* [10] observed Hong-Ou-Mandel (HOM) two-photon interference of statistically distributed photons generated via spontaneous parametric down-conversion. Although few proof-of-principle experiments exploited this valuable type of PNR detector [11], TES-based systems are still rarely applied in the wide and active field of solid-state based non-classical light sources.

In this work, we employ PNR detectors based on tungsten TESs for the quantum metrology of triggered single-photon sources (SPSs). We directly observe HOM two-photon interference at a beamsplitter. Offering quantum efficiencies close to unity and true PNR-capability, the TES-based two-channel detector allows us to analyse the photon-number distribution as well as the photon indistinguishability of our quantum-light source. Additionally, we quantitatively compare the results of the PNR experimtents with reference data obtained with conventional click detectors in Hanbury Brown and Twiss-(HBT-) and HOM-configuration.

2. Single-photon source and experimental setup

In this section, the utilized SPS is briefly discussed (section 2.1) followed by a description of the experimental configuration including the PNR detection system (section 2.2). To perform quantum metrology of our SPS, we combine a micro-photoluminescense setup with photon statistics measurements using a PNR detection system in HBT- as well as HOM-type configuration. Additionally, standard click detectors are used for comparative reference measurements.

2.1. Sample technology

The non-classical light source used in our experiments is represented by a deterministically fabricated quantum dot (QD) based SPS. This type of SPS was previously exploited to demonstrate the efficient generation of indistinguishable single photons [12], twin-photon states [13], and polarization entangled photon pairs [14]. The device is based on a single pre-selected InGaAs QD embedded precisely at the center of a monolithic microlens made out of GaAs. Together with a distributed Bragg reflector (AlGaAs/GaAs) beneath the QD, this photonic nanostructure enhances the photon extraction efficiency of the emitter to typical values of 20%–30% into a numerical aperture (NA) of 0.4. For the deterministic fabrication of the QD-microlens aligned to a pre-selected target emitter, we employed a technique called 3D *in situ* electron-beam lithography. For a detailed review on this type of quantum light source, we refer the reader to [15].

2.2. Basic experimental setup

The experimental setups used for optical quantum metrology are illustrated in figure 1(a). A confocal micro-photoluminescence (μPL) setup is employed, with the sample mounted onto the cold finger of a Helium-flow cryostat at a temperature of 8 K. The sample is excited using a pulsed wavelength-tunable titanium-sapphire (Ti:Sa) laser operated in ps-mode (repetition rate: 80 MHz) at a wavelength of 909 nm, corresponding to p-shell excitation of the QD. PL from the QD microlens is collected via a microscope objective (NA: 0.4) and spectrally analysed using a monochromator with attached charge-coupled device camera (overall spectral resolution: 0.017 nm/25 μeV). For photon statistics experiments, the emission of the charge-neutral QD exciton X^0 is spectrally filtered using the exit slit of the monochromator (100 μeV bandwidth) and then coupled either to a fiber-based HBT- or HOM-type setup. In case of the HBT experiment the QD is excited using laser pulses with a period of 12.5 ns (see figure 1(a), inset). The resulting emission of the X^0-state leaving the monochromators' exit slit is coupled to a 50:50 beamsplitter based on optical multimode fibers. Both output ports of the beamsplitter are then coupled either to the PNR detection system (see section 2.3) or standard click detectors (SPCMs). In case of the HOM experiments, the QD is excited using a sequence of double-pulses with a pulse-separation of 4 ns. The resulting emission of the X^0-state is coupled to a fiber-based polarization-maintaining asymmetric Mach–Zehnder interferometer attached to the output port of the monochromator. The polarization of the photons in one interferometer arm can be switched, either being co- or cross-polarized with respect to the other arm. The interference of consecutively emitted photons at the second beam-splitter is ensured by a 4 ns delay-line in one interferometer arm. Details on the HOM-setup can be found in [16]. At the two output ports of the HOM-setup photons are again detected using PNR or click detectors, respectively. To obtain reference measurements for the second-order photon autocorrelation as well as the photon indistinguishability (see section 3.1), the HBT and HOM setup are used in combination with the click detectors based on silicon avalanche photo diodes with an overall timing resolution of 350 ps in combination with time-correlated single-photon counting electronics.

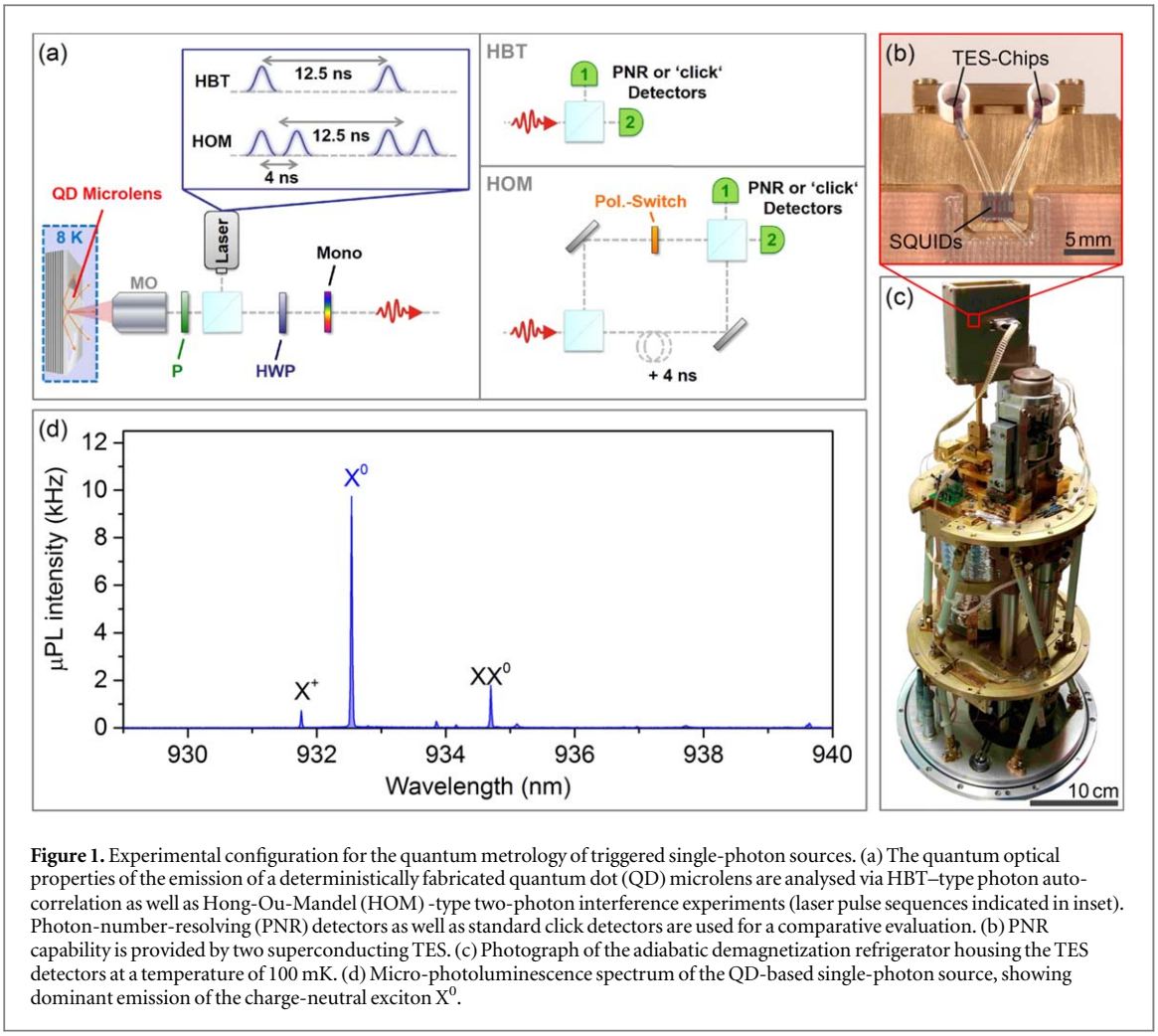

Figure 1. Experimental configuration for the quantum metrology of triggered single-photon sources. (a) The quantum optical properties of the emission of a deterministically fabricated quantum dot (QD) microlens are analysed via HBT–type photon auto-correlation as well as Hong-Ou-Mandel (HOM) -type two-photon interference experiments (laser pulse sequences indicated in inset). Photon-number-resolving (PNR) detectors as well as standard click detectors are used for a comparative evaluation. (b) PNR capability is provided by two superconducting TES. (c) Photograph of the adiabatic demagnetization refrigerator housing the TES detectors at a temperature of 100 mK. (d) Micro-photoluminescence spectrum of the QD-based single-photon source, showing dominant emission of the charge-neutral exciton X^0.

2.3. Photon-number-resolving detection system

PNR experiments are enabled by employing a two-channel detection system based on fiber-coupled tungsten TESs operated in a cryogenic environment. Each of the TESs acts as a highly sensitive calorimeter, which is able to detect smallest amounts of energy dissipated during photon absorption. The energy dissipation results in a rise of temperature, which ultimately leads to a detectable change in electrical current. The latter is measured via an inductively coupled two-stage direct-current superconducting quantum interference device (SQUID). The TES/SQUID detector units are mounted onto the cold stage of an adiabatic demagnetization refrigerator stabilized at a temperature of 100 mK. This compact custom-made state-of-the-art detection system enables detections efficiencies of >87% in the spectral region of interest (850–950 nm) and discriminates photon numbers of up to 25. A detailed characterization of the PNR detection system is reported in [17]. For the PNR experiments, it was additionally necessary to reduce the excitation repetition rate to 1 MHz by pulse picking the excitation laser (80 MHz repetition rate), to accommodate for the thermal recovery time (~1 μs) of the TES chips. To achieve the required suppression between picked pulses, we applied a two-stage pulse-picking scheme as follows. First, an acousto-optical modulator (AOM) is synchronized to the pulsed Ti:Sa laser to diffract every 80th pulse into 1st order. The AOM shows an overall extinction ratio of >1/2000, yet the subsequent pulse of the picked one is only suppressed by a factor of ~50, due to the finite decay time constant of the AOM. For this reason, a fiber-coupled electro-optical modulator is added as second pulse-picking stage to prevent re-excitation of the quantum emitter. Carefully matching the time windows of the two modulators results in an overall extinction ratio of >1/10000 and a suppression of the subsequent pulse of >200, which is sufficient for the experiments in this work. The resulting laser pulses are then coupled to a fiber-based asymmetric Mach–Zehnder interferometer forming the final pulse sequence, launching a double-pulse (4 ns pulse-separation) every 1 μs to the sample.

3. Quantum metrology of solid-state single-photon sources

The quantum optics experiments conducted in the following are of fundamental importance in quantum optics and metrology. The HBT experiment provides access to the second-order photon auto-correlation function

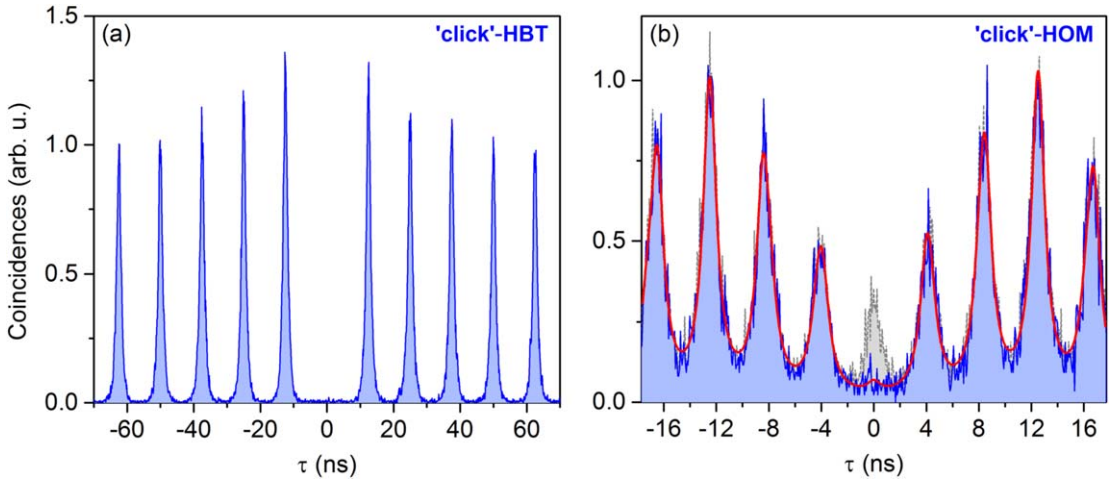

Figure 2. Photon statistics measurements on the emission of the SPS using standard click detectors based on avalanche photon diodes. (a) Measured second-order photon auto-correlation $g^{(2)}(\tau)$ of a QD-microlens demonstrating strong suppression of two photon emission events with $g^{(2)}_{\mathrm{HBT,\,click}}(0) = 0.035 \pm 0.003$. (b) HOM–type two-photon interference experiment carried out with the setup in figure 1(a). Experimental data for co- (solid, blue line) and cross- (dashed) polarized photons are shown together with a fit (solid, red line) for the co-polarized measurement. A photon-indistinguishability of $V_{4\mathrm{ns}} = (90 \pm 5)\%$ is determined.

$g^{(2)}{}_{\mathrm{HBT}}(\tau)$ and reveals the sub-Poissonian statistics of non-classical light sources. This enables us to determine the suppression of multi-photon emission events, which is of great importance for quantum-secured communication using quantum-light sources [18, 19]. In contrast, the HOM experiment reveals the indistinguishability of photons emitted by one or multiple light sources [20]. Thereby, the photon indistinguishability represents the crucial parameter for many applications in quantum information processing [21]. In section 3.1 we will first present reference measurements of both quantities using standard single-photon click detectors, before we demonstrate the corresponding measurements employing our detectors with photon-number resolution in section 3.2.

3.1. Reference experiments using 'click' detectors

To classify the experiments exploiting the photon-number resolution of our TES-based detector system presented in section 3.2, we performed measurements with click detectors for reference. Figure 2(a) depicts the corresponding measurement data of the second-order photon-autocorrelation $g^{(2)}{}_{\mathrm{HBT}}(\tau)$. Almost negligible coincidences at $\tau = 0$ proof pronounced single-photon emission. A quantitative analysis of the experimental data reveals $g^{(2)}{}_{\mathrm{HBT,click}}(0) = 0.035 \pm 0.003$. Next, we address the photon-indistinguishability in HOM-type experiments using click detectors. Figure 2(b) displays the obtained coincidence histograms of two-photon detection events at the output ports of the HOM setup. In case of co-polarized photons (solid blue curve), quantum-mechanical two-photon interference manifests in a strongly reduced number of coincidences at $\tau = 0$, compared to the measurement in cross-polarized configuration (dashed gray curve). Quantitatively evaluating the experimental data for co-polarized measurement configuration according to [16], we extract a two-photon interference visibility of $V_{\mathrm{HOM,click}} = (90 \pm 5)\%$.

3.2. Photon-number-resolving experiments

For the quantum metrology with photon-number resolution, we use the PNR detector system described in section 2.3 with the experimental configuration displayed in figure 1(a). This experimental configuration allows us to measure the number of photons at the two output ports of the HOM setup, providing direct access to the result of the two-photon interference experiment. Due to the limited temporal resolution (~1 μs) of the PNR detectors, and in contrast to the corresponding experiment with click detectors, the different pathway combinations of two photons resulting from one excitation cycle cannot be distinguished. Therefore we evaluate the correlated photon-number-distribution of either measuring one or two photons at each channel of the PNR detector. From this measurement we deduce the conditional probability $P(\mathrm{TES}_1, \mathrm{TES}_2)$ to detect n photons in TES detectors 1 and 2 in co-polarized and cross-polarized configuration. Out of four possible pathway combinations at the first beam splitter, only one allows the two photons to arrive simultaneously and interfere at the second beam splitter. This is comparable to the central peak of the cluster at zero-delay in figure 2(b). For cross-polarized configuration the probabilities to measure one photon in each output port $P(1/1)$ or to measure two photons at either output port $P(2/0, 0/2)$ are equally distributed, as the photons are distinguishable, leaving the Mach–Zehnder interferometer statistically uncorrelated. For co-polarized configuration, however, the probability $P(2/0, 0/2)$ is enhanced while

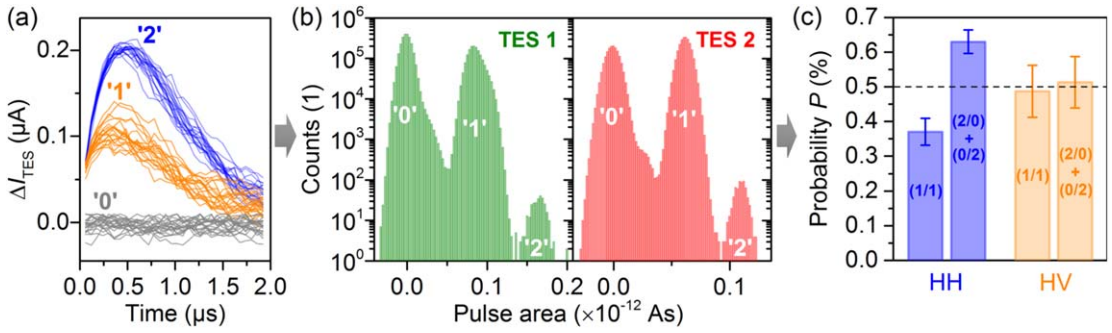

Figure 3. Photon statistics measurements using a TES-based two-channel detector system providing true photon-number-resolution in a HOM-type setup. (a) Time traces showing the change in TES current ΔI_{TES} during zero- ('0'), single- ('1') and two- ('2') photon detection events. (b) Pulse-area-distributions of time traces recorded with TES 1 and TES 2 at the output ports of the HOM interferometer for co-polarized (HH) measurement setting. (c) Conditional probabilities P(TES 1, TES 2) of detecting n photons at TES 1 and TES 2 extracted from the PNR HOM experiment in co-polarized (HH) and cross-polarized (HV) measurement setting. Error bars correspond to one standard deviation deduced from the raw detection events assuming a Poissonian distribution.

the $P(1/1)$ is reduced. The resulting contrast $\frac{P(2/0,0/2)}{P(1/1)} = \frac{\eta_1^2+\eta_2^2}{2\eta_1\eta_2} \times \frac{(3/4+u)}{(5/4-u)}$ reveals the degree of photon-indistinguishability $V_{HOM} = 4u - 1$, where a finite detection efficiency mismatch η_1/η_2 between the two detection channels is taken into account. Note, that in cases of reasonably high detection efficiencies (>30%), it is sufficient to consider the easily accessible efficiency mismatch η_1/η_2, although the visibility depends on the absolute values of η_1 and η_2.

In our PNR experiment, we record the time traces of the response of both TES/SQUID detector units, which are coupled to the HOM experiment via single-mode fibers. Examples of time traces recorded in the co-polarized (HH) configuration are displayed in figure 3(a). The conditional probabilities described above are evaluated, by post-selecting pairs of traces at TES 1 and TES 2 from the raw data corresponding to events (1/1), (2/0) and (0/2). For this purpose we analyse the pulse area of measured time traces. It is worth mentioning, that other methods for evaluating the time traces are possible, such as the principal component analysis or simply the pulse height [17]. In this case, the pulse-area analysis in combination with moderate constraints to the pulse shape (i.e. slope of rising/falling edge) enabled the optimum performance in terms of energy resolution and efficient filtering of erroneous events due to 'pile-ups' of consecutive photons or 'cosmics'. Figure 3(b) depicts count histograms of the pulse area extracted from time traces of both TES units in HH configuration. The occurrence of zero ('0'), one ('1') and two-photon ('2') detection events is clearly discriminated, demonstrating the high energy resolution of our TESs. Note, that the overlap between the peaks of the photon number states is only visible in logarithmic scaling, which was chosen in order to show the two-photon events more clearly. The corresponding conditional propabilities are dipicted in figure 3(c) for HH- and HV-configuration, respectively, where error bars correspond to one standard deviation. For HH setting, the probability $P(2/0, 0/2)$ to detect a photon pair at one of the two HOM output ports is significantly increased, while the probability $P(1/1)$ to detect single photons at both TESs is reduced with respect to the probabilistic case (indicated as dashed line). This observation confirms the presence of quantum mechanical two-photon interference of indistinguishable photons at the HOM beamsplitter. For HV setting, i.e. distinguishable photons at the HOM beamsplitter, the probabilities $P(1/1)$ and $P(2/0, 0/2)$ are the same within the measurement error. Taking into account the observed detection efficiency mismatch of the two detection channels $\eta_1/\eta_2 = 0.68$ and using the formula discussed above, we determine a photon-indistinguishability of $V_{HOM,PNR} = (90 \pm 7)\%$. In addition, we also perform and analyse PNR measurements in HBT-configuration to access the suppression of two-photon emission events of our SPS. Using the approximation $g^{(2)}_{HBT}(0) \approx 2P_2/P_1{}^2$ [22], where P_n is the probability to detect n photons, we gain the antibunching value $g^{(2)}_{HBT,PNR}(0) = 0.08 \pm 0.02$ of our PNR experiment.

4. Discussion and conclusion

The experimental results obtained in our work using PNR as well as click detectors in HBT- and HOM-configuration are comparatively summarized in table 1. The observed photon indistinguishabilities are in excellent quantitative agreement for both measurement techniques. In addition, both experimental values for the antibunching are well below 10%, but the best value is slightly higher in case of the PNR experiment. This is consistent with a reduction of the signal-to-noise ratio in the spectra of our SPSs, when switching from 80 to 1 MHz excitation repetition rate, which increases the measured $g^{(2)}(0)$ value [23]. The aquisition time for the

Table 1. Summary of quantum metrology experiments using click- and PNR-detectors. Measured quantities are the antibunching $g^{(2)}_{\mathrm{HBT}}(0)$ and the photon-indistinguishability V_{HOM}.

Quantity	'Click'-detectors	PNR-detectors
$g^{(2)}_{\mathrm{HBT}}(0)$	0.035 ± 0.003	0.08 ± 0.02
V_{HOM}	$(90 \pm 5)\%$	$(90 \pm 7)\%$

PNR measurements presented in figure 3 was 288 min for the HOM and 212 min for the HBT experiment. In case of the measurements using click detectors, we integrated coincidences for 49 and 57 min for the HOM and HBT experiment, respectively. The thermal recovery time ($\sim$1 μs) of TES-based PNR detectors is probably the only drawback compared to fast state-of-the-art click detectors based on avalanche photo diodes or superconducting nanowire detectors. However, this thermal recovery time can be improved at least to a certain extend by engineering the thermal coupling between the electron and phonon system of the TES [24]. On the other hand, the advantage of TES-based detectors is clearly the intrinsic PNR-capability with large detection efficiencies. Using spatially multiplexed click detectors with beamsplitters, for instance, the efficiency to detect an n-photon state quickly degrades with n, while the corresponding PNR measurement yields the same detection efficiency η largely independent of n. Thus, while the present proof-of-principle experiments (limited to $n = 1, 2$) did not fully exploit the potential of PNR detectors in terms of the required measurement time, clear advantages are expected for experiments utilizing multi-photon states with higher n, such as photonic boson sampling [25, 26] or multi-partite entanglement [27]. More generally, any experiment where the involved photon numbers are not known beforehand are not faithfully possible using click detectors. This is for instance the case for mixtures of thermal and coherent light states emitted by QD-microlasers [28] or exciton-polariton condensates in microcavities [29], for which our TES detection system has been employed recently.

In summary, we employed a state-of-the-art PNR detector system for the quantum metrology of solid-state single-photon sources. The two-channel PNR detector system is based on superconducting tungsten TESs, which we used to evaluate the photon indistinguishability as well as the multi-photon supression, both representing crucial characteristics for applications in photonic quantum information processing. Additionally, we perform reference measurements using standard click detectors in HBT- and HOM- configuration. The photon indistiguishability of $(90 \pm 7)\%$ observed in our PNR experiments, is in excellent agreement with the value obtained in the HOM experiment with click detectors. Our work demonstrates that TES-based detectors, offering true photon-number-resolution and high detection efficiency, are perfectly suitable for the quantum metrology of non-classical light sources and show up a promising route towards efficient implementations of quantum information tasks based on multi-photon states.

Acknowledgments

We acknowledge support from the German Research Foundation (DFG) via the SFB 787 'Semiconductor Nanophotonics: Materials, Models, Devices' and Grant RE2974/18-1, the German Federal Ministry of Education and Research (BMBF) via the VIP-project QSOURCE (Grant No. 03V0630). Parts of the results in this paper come from the project EMPIR 14IND05 MIQC2. This project has received funding from the EMPIR programme co-financed by the Participating States and from the European Union's Horizon 2020 research and innovation programme. T H gratefully acknowledges funding of the German Federal Ministry of Education and Research (BMBF) via the project 'QuSecure' (Grant No. 13N14876) within the funding program Photonic Research Germany. We thank A E Lita and S W Nam for providing the TES detector chips.

ORCID iDs

Tobias Heindel https://orcid.org/0000-0003-1148-404X
Stephan Reitzenstein https://orcid.org/0000-0002-1381-9838

References

[1] Acin A *et al* 2018 The quantum technologies roadmap: a European community view *New J. Phys.* **20** 080201
[2] Aharonovich I *et al* 2016 Solid-state single-photon emitters *Nat. Photon.* **10** 631
[3] Chunnilall C *et al* 2014 Metrology of single-photon sources and detectors: a review *Opt. Eng.* **53** 081910
[4] Rodiek B *et al* 2017 Experimental realization of an absolute single-photon source based on a single nitrogen vacancy center in a nanodiamond *Optica* **4** 71

[5] Heilmann R et al 2016 Harnessing click detectors for the genuine characterization of light states Sci. Rep. 6 19489
[6] Thomay T et al 2017 Simultaneous, full characterization of a single-photon state Phys. Rev. X 7 041036
[7] Hadfield R H 2009 Single-photon detectors for optical quantum information applications Nat. Photon. 3 696
[8] Eisaman M D, Fan J, Migdall A and Polyakov S V 2011 Single-photon sources and detectors Rev. Sci. Instrum. 82 071101
[9] Lita A E, Miller A J and Nam S W 2008 Counting near-infrared single-photons with 95% efficiency Opt. Express 16 3032
[10] Di Giuseppe G et al 2003 Direct observation of photon pairs at a single output port of a beam-splitter interferometer Phys. Rev. A 68 063817
[11] Gerrits T et al 2016 Superconducting transition edge sensors for quantum optics superconducting devices in quantum optics Superconducting Devices in Quantum Optics ed R H Hadfield and G Johansson (Cham, Switzerland: Springer International Publishing) pp 31–60
[12] Gschrey M et al 2015 Highly indistinguishable photons from deterministic quantum-dot microlenses utilizing three-dimensional in situ electron-beam lithography Nat. Commun. 6 7662
[13] Heindel T et al 2017 A bright triggered twin-photon source in the solid state Nat. Commun. 8 14870
[14] Bounouar S et al 2018 Generation of maximally entangled states and coherent control in quantum dot microlenses Appl. Phys. Lett. 112 153107
[15] Heindel T, Rodt S and Reitzenstein S 2017 Single-Photon Sources Based on Deterministic Quantum-Dot Microlenses, in Quantum Dots for Quantum Information Technologies ed P Michler (Cham, Switzerland: Springer International Publishing) pp 199–232
[16] Thoma A et al 2016 Exploring dephasing of a solid-state quantum emitter via time-and temperature-dependent Hong-Ou-mandel experiments Phys. Rev. Lett. 116 033601
[17] Schmidt M et al 2018 Photon-number-resolving transition-edge sensors for the metrology of quantum light sources J. Low Temp. Phys. 193 1243
[18] Waks E et al 2002 Security aspects of quantum key distribution with sub-poisson light Phys. Rev. Lett. 66 42315
[19] Heindel T et al 2012 Quantum key distribution using quantum dot single-photon emitting diodes in the red and near infrared spectral range New J. Phys. 14 83001
[20] Thoma A 2017 Two-photon interference from remote deterministic quantum dot microlenses Appl. Phys. Lett. 110 011104
[21] Santori C et al 2002 Indistinguishable photons from a single-photon device Nature 419 594
[22] Scarani V et al 2009 The security of practical quantum key distribution Rev. Mod. Phys. 81 1301
[23] Brouri R et al 2000 Photon antibunching in the fluorescence of individual color centers in diamond Opt. Lett. 25 1294
[24] Calkins B et al 2011 Faster recovery time of a hot-electron transition-edge sensor by use of normal metal heat-sinks Appl. Phys. Lett. 99 241114
[25] Loredo J C et al 2017 Boson sampling with single-photon fock states from a bright solid-state source Phys. Rev. Lett. 118 130503
[26] Wang H et al 2017 High-efficiency multiphoton boson sampling Nat. Photon. 11 361
[27] Pan J-W et al 2012 Multiphoton entanglement and interferometry Rev. Mod. Phys. 84 777
[28] Schlottmann E et al 2018 Exploring the photon-number distribution of bimodal microlasers with a transition edge sensor Phys. Rev. Appl. 9 064030
[29] Klaas M et al 2018 Photon-number-resolved measurement of an exciton-polariton condensate Phys. Rev. Lett. 121 047401